3,3-Bis(3,5-dimethylpyrazol-1-yl)propionic acid: A tripodal *N,N,O* ligand for manganese and rhenium complexes – Syntheses and structures

Liv Peters [a], Eike Hübner [a], Thomas Haas [b], Frank W. Heinemann [a], Nicolai Burzlaff [a,*]

[a] *Department of Chemistry and Pharmacy & Interdisciplinary Center for Molecular Materials (ICMM), University of Erlangen-Nürnberg, Egerlandstraße 1, D-91058 Erlangen, Germany*
[b] *Department of Chemistry, University of Konstanz, Fach M728, 78457 Konstanz, Germany*

ABSTRACT

The tripodal *N,N,O* ligands 3,3-bis(3,5-dimethylpyrazol-1-yl)propionic acid (Hbdmpzp) (**1**) and 3,3-bis(pyrazol-1-yl)propionic acid (Hbpzp) (**2**) form the "missing link" between the well-known bis(pyrazol-1-yl)acetic acids and related ligands with a longer "carboxylate arm". To illustrate the reactivity of this ligand, manganese and rhenium complexes bearing the ligand bdmpzp are reported. The complexes are compared to related compounds bearing other tripod ligands such as bis(3,5-dimethylpyrazol-1-yl)acetate (bdmpza) and 3,3-bis(1-methylimidazol-2-yl)propionate (bmip). Spectroscopic and structural data are used as a basis for comparison, as well as DFT calculations. Both ligands **1** and **2** and the complexes *fac*-[Mn(bdmpzp)(CO)₃] (**3**) and *fac*-[Re(bdmpzp)(CO)₃] (**4**) were characterised by X-ray crystallography.

© 2009 Elsevier B.V. All rights reserved.

1. Introduction

Bis(3,5-dimethylpyrazol-1-yl)acetic acid (Hbdmpza), first introduced into coordination chemistry by Otero in 1999, has been successfully employed in the synthesis of coordination compounds with many transition metals of the periodic system [1–3]. Especially the tricarbonyl complexes *fac*-[Mn(bdmpza)(CO)₃] and *fac*-[Re(bdmpza)(CO)₃] and the trioxo complex *fac*-[Re(bdmpza)O₃] attracted some interest for their possible application for radiopharmaceutical purposes [4,5]. Very recently, the analogous complex *fac*-[Tc(bpza)O₃] (bpza: bis(pyrazol-1-yl)acetate) was published by Tooyama and co-workers [6]. In 2004 two ligands very similar to Hbdmpza were synthesised by Díez-Barra et al., namely sodium 3,3-bis(pyrazol-1-yl)propionate (Na[bpzp]) and sodium 3,3-bis(3,5-dimethylpyrazol-1-yl)propionate (Na[bdmpzp]) (Fig. 1) [7]. So far, no complexes bearing these ligands have been reported. 3,3-Bis(pyrazolyl-1-yl)propionic acid and 3,3-bis(3,5-dimethylpyrazol-1-yl)propionic acid may serve as a "missing link" in the comparison of bis(pyrazol-1-yl)acetic acids and facially coordinating *N,N,O* ligands with a longer "carboxylate arm" such as 3,3-bis(1-methylimidazol-2-yl)propionic acid (Na[bmip]) (Fig. 1) [11] and should provide arguments in the discussion whether a longer "carboxylate arm" makes a difference to the coordination properties of the ligand or not. Furthermore, also these ligands might

be of use in the search for new rhenium and technetium radiopharmaceutics.

Here we report on the preparation of the free acids 3,3-bis(3,5-dimethylpyrazol-1-yl)propionic acid (Hbdmpzp) (**1**) and 3,3-bis(pyrazol-1-yl)propionic acid (Hbpzp) (**2**). We also synthesised the – to the best of our knowledge – first complexes with a κ³-bound bdmpzp ligand. Manganese and rhenium tricarbonyl complexes were chosen as a first synthetic target, because the CO vibrations, which can be monitored by IR spectroscopy, are a good probe for the electron donating or accepting properties of the ligand. Furthermore, the IR and X-ray data of analogous complexes with bis(pyrazol-1-yl)acetato ligands are already available for a comparison [4]. As a third argument for the synthesis of these complexes may serve their possible use in the search for new rhenium and technetium radiopharmaceutics. Besides the *fac*-[M(CO)₃]⁺-core (M = Re, Tc) the metal fragments [M(CO)₂(NO)]²⁺ and [MO₃]⁺ (M = Re, Tc) are subjects of current radiopharmaceutics research [6,8]. 3,3-Bis(3,5-dimethylpyrazol-1-yl)propionato complexes with these fragments will be discussed, as well.

2. Results and discussion

2.1. DFT calculations

To gain first insights into the similarities and differences of the coordination behaviour of various ligands, the dissociation energy of the following theoretical reaction was calculated for several

* Corresponding author. Tel.: +49 (0)9131 85 28976; fax: +49 (0)9131 85 27387.
E-mail address: burzlaff@chemie.uni-erlangen.de (N. Burzlaff).

bpza: R = H
bdmpza: R = CH$_3$

bpzp: R = H
bdmpzp: R = CH$_3$

bip: R = H
bmip: R = CH$_3$

Cp: R = H
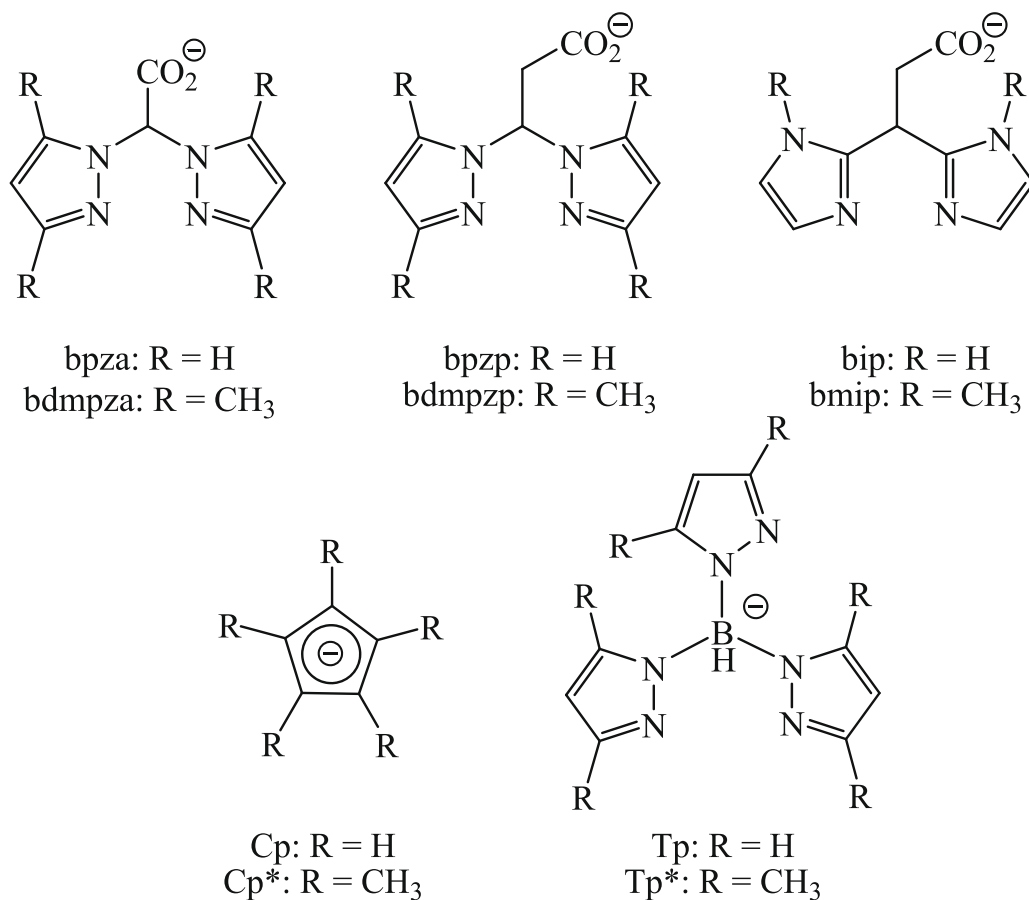Cp*: R = CH$_3$

Tp: R = H
Tp*: R = CH$_3$

Fig. 1. The ligands bdmpza, bpza, bpzp, bdmpzp, bmip, bip, Cp, Cp*, Tp and Tp*.

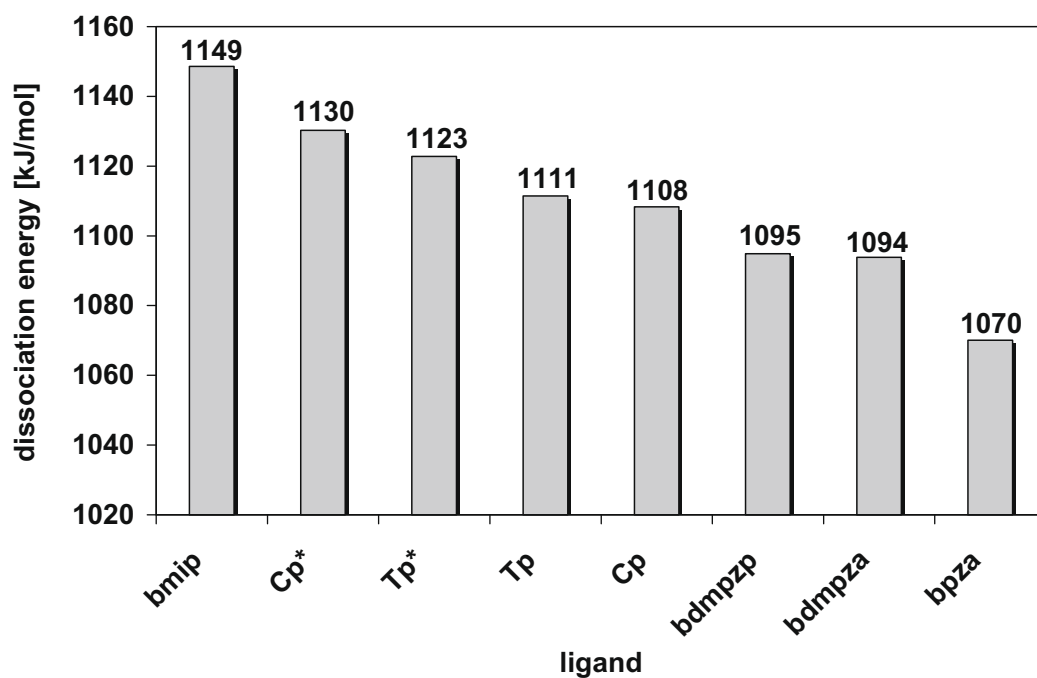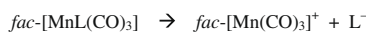**Fig. 2.** Calculated dissociation energies.

ligands L (L = bpza, bdmpza, bdmpzp, Tp, Tp*, Cp, Cp*, bmip) (Figs. 1 and 2, Eq. (1)):

$$fac\text{-}[MnL(CO)_3] \rightarrow fac\text{-}[Mn(CO)_3]^+ + L^-$$

Eq. (1). *In silico* dissociation experiment.

To obtain the relative energies of the dissociation reactions, the hybrid functional B3P86 was used. We calculated the unrelaxed dissociation energy, i.e., the metal complex was fully geometry-optimised and subsequently resolved into its fragments. The energy of the fragments was obtained by single-point calculations without geometry-optimisation. Thus, only information about the interaction of the ligand with the metal fragment was obtained, and possible interferences by stabilisation of the ligand through intramolecular H-bonds, etc. could be excluded. In a comparative analysis of several platinum complexes Harvey was able to establish a relation between σ- and π-donation and π-backdonation and the dissociation energy. He found, that the over-all bond energy often correlates to the sum of the σ- and π-interactions, but does not always consist solely of the sum of these effects [9]. Thus, in order to obtain comparable results, we restricted our study to tripodal monoanionic ligands bound to a *fac*-[Mn(CO)₃] fragment. The calculated values for the dissociation energies in this purely hypothetic reaction do of course not correlate with any complex formation constant. The values represent the sum of all possible influences and might allow to decide beforehand, which ligand could be a promising synthetic target for a specific application.

According to our calculations (Fig. 2) the dissociation energy of 3,3-bis(3,5-dimethylpyrazol-1-yl)propionate (bdmpzp) remains practically unchanged compared to bis(3,5-dimethylpyrazol-1-yl)acetate (bdmpza) despite the additional CH₂ group. This implies that the coordination properties of a bdmpza ligand should be very similar compared to bdmpza, although it comprises a longer "carboxylate arm". Nevertheless, this hypothesis had to be proven by spectroscopical and structural data of actual complexes.

Furthermore, bdmpzp forms the "missing link" between the bdmpza and the bmip ligand for which the calculated dissociation energy is by far higher (Fig. 2). Thus, the result discussed above enables a decision on whether this large difference between bdmpza and bmip has to be attributed to the different N donors or also to the length of the "carboxylate arm". Obviously and already proven by the discussion of the calculated frontier orbitals and the IR spectra of the complexes *fac*-[Mn(bmip)(CO)₃] and *fac*-[Re(bmip)(CO)₃], complexes containing imidazolyl N donors are very different from complexes with pyrazolyl N donors [10,11]. Orbital calculations show that pyrazole-containing N,N,O ligands are σ- and π-donors but also π-acceptor ligands [11], whereas for imidazole based ligands the metal interaction is based mainly on their σ- and π-donor properties, which is only slightly weakened by CO π-acceptors in *trans*-position. This might explain the higher calculated dissociation energy.

A third aspect, which can be derived from our *in silico* experiment, is related to the electron donating properties of the ligand towards the metal fragment. In short it can be said for an *fac*-[Mn(CO)₃]⁺ fragment, that the more electron donating the ligand, the higher is the dissociation energy. This can be shown by the comparison of bdmpza to bpza, since the methyl groups enhance the electron donating properties, as can be seen by the IR spectra of *fac*-[Mn(bpza)(CO)₃] and *fac*-[Mn(bdmpza)(CO)₃] (Table 3) [4,11]. In the same way, the dissociation energy of bdmpza is higher than that of bpza, even though steric interactions would suggest an opposite effect. The same tendency can be seen in the comparison of Tp to Tp* and of Cp to Cp* (Fig. 2). The comparison between Tp, Cp and bdmpza in terms of their calculated dissociation energies should be considered cautiously, due to different electrostatic interactions.

2.2. Syntheses and X-ray structures of the ligands

The synthesis of 3,3-bis(3,5-dimethylpyrazol-1-yl)propionic acid (Hbdmpzp) (**1**) and 3,3-bis(pyrazol-1-yl)propionic acid (Hbpzp) (**2**) followed the procedure described in the literature for sodium 3,3-bis(3,5-dimethylpyrazol-1-yl)propionate and sodium 3,3-bis(pyrazol-1-yl)propionate. These ligands are synthesised by an entirely different pathway than bis(pyrazol-1-yl)acetic acids. For the latter the pyrazole moieties are either bridged to a methane and subsequently the "carboxylate arm" is attached to the bridging carbon atom, or they are reacted with dibromo- or dichloroacetic acid. Now, these two ligands are prepared in a double Michael addition of the deprotonated pyrazoles to methyl propiolate [7]. Instead of the workup described in the literature we chose an aqueous–acidic workup to obtain the free acids **1** and **2** in moderate to good yields (Eq. (2)).
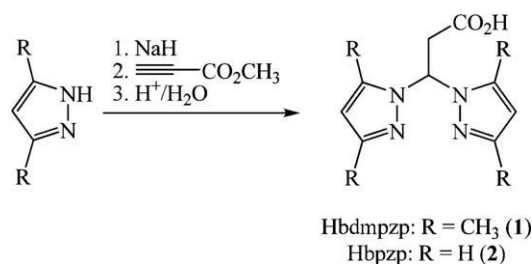

Eq. (2). Synthesis of the ligands Hbdmpzp (**1**) and Hbpzp (**2**).

The formation of **1** is detected by NMR spectroscopy. The signal of the proton at the bridging carbon atom is split into a triplet (δ = 6.72 ppm, $^3J_{H,H}$ = 6.8 Hz), and the protons of the CH₂ group show a doublet (δ = 3.63 ppm, $^3J_{H,H}$ = 6.8 Hz). Furthermore, the presence of the carboxylate group is indicated by a resonance at 171.2 ppm in the ¹³C NMR spectrum. The formation of **1** is further confirmed by a [M+H⁺] peak in the mass spectrum and by the detection of the asymmetric carboxylate vibration in the IR spectra at 1711 cm⁻¹ (KBr) and 1735 cm⁻¹ (THF). Compound **2** shows the same characteristic features of the ligand. The resonance of the proton at the bridging carbon atom is detected as a triplet at δ = 6.93 ppm ($^3J_{H,H}$ = 7.4 Hz), and the protons of the CH₂ group appear as a doublet at δ = 3.66 ppm ($^3J_{H,H}$ = 7.4 Hz). Again the mass spectrum (m/z = 207 [M+H⁺]) and the IR spectra supply more evidence for the formation of **2**. Here, the asymmetric vibration band of the carboxylate group is detected at 1709 cm⁻¹ (KBr) and 1741 cm⁻¹ (THF). From both compounds crystals suitable for X-ray structure determinations were obtained by crystallisation from acetone (see Supporting Material). Bond distances and angles of **1** and **2** are very similar to each other and also in good agreement with those reported earlier for similar ligands [12–14].

2.3. Syntheses of the complexes

Since the binding properties of bdmpzp, bpzp and other known tripod ligands such as bdmpza, bpza, Tp and Tp* are best compared by IR spectroscopy and single crystal X-ray diffraction, we prepared manganese and rhenium tricarbonyl complexes of bdmpzp. Complexes were synthesised by analogy to *fac*-[M(bdmpza)(CO)₃] (M = Mn, Re), starting from the potassium salt of **1** and the pentacarbonyl complexes [MnBr(CO)₅] and [ReBr(CO)₅] (Eq. (3)) [4]. When the same synthesis was attempted with the potassium salt of **2** and [MBr(CO)₅] (M = Mn, Re), only insoluble products were obtained, which could not be analysed further, so far.
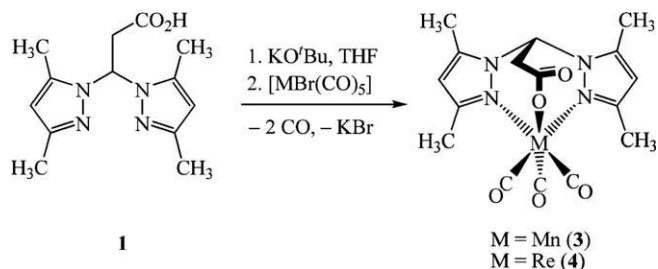
Eq. (3). Synthesis of the complexes *fac*-[M(bdmpzp)(CO)₃] (M = Mn, Re) (**3**, **4**).

The progress of the reactions can be monitored by IR spectroscopy due to the intense characteristic signals of the carbonyl residues. In contrast to *fac*-[M(bdmpza)(CO)₃] and *fac*-[M(bpza)(CO)₃] (M = Mn, Re), the complexes **3** and **4** precipitate as the reaction proceeds. Complexes **3** and **4** were isolated by filtration, and KBr was removed from the products by washing with degassed water. The solubility of **3** and **4** (soluble in methanol, insoluble in THF) resembles rather that of *fac*-[M(bmip)(CO)₃] (M = Mn, Re) than that of *fac*-[M(bdmpza)(CO)₃] (M = Mn, Re). Both complexes are stable as solids under aerobic conditions. Only **3** tends to decompose when kept in solution. The two pyrazolyl groups in the complexes are chemically equivalent, showing only one set of signals in the NMR spectra. The signals in the ^{1}H NMR spectra of **3** are broad. The ^{13}C NMR spectrum of **4** exhibits two signals for the carbonyl ligands at a ratio of 2:1 (**4**: δ = 196.3 and 196.5 ppm). In the ^{13}C NMR spectrum of **3** not all signals can be observed. The carboxylate group is only detected in the spectrum of **4** at 172.1 ppm in CDCl₃ and 171.4 ppm in DMSO-d_6. Crystals suitable for X-ray structure determinations of *fac*-[Mn(bdmpzp)(CO)₃] (**3**) and *fac*-[Re-(bdmpzp)(CO)₃] (**4**) were obtained from solutions in methanol/water (Figs. 3 and 4). Selected bond lengths and angles are summarised in Table 1.

Both compounds **3** and **4** show C_s symmetry. The "carboxylate arm" lies in the mirror plane of the complex. The same symmetry was found in the complexes *fac*-[M(bdmpza)(CO)₃] (M = Mn, Re) and *fac*-[M(bmip)(CO)₃] (M = Mn, Re) [4,11]. On the contrary, in complexes in which the bdmpza ligand bears a second substituent at the bridging carbon atom, the carboxylate donor group is bent out of the mirror plane [15]. In the complexes **3** and **4** the bond distances between the metal atom and the carbonyl ligands *trans* to the pyrazole groups are very similar to those reported for *fac*-[M(bdmpza)(CO)₃] (M = Mn, Re) and *fac*-[M(bmip)(CO)₃] (M = Mn,
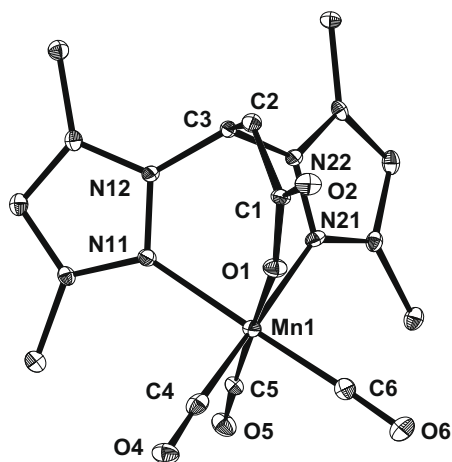
Re) [4,11]. Both bonds are longer than the metal–carbonyl distance M1–C5 *trans* to the carboxylate group. This is due to the *trans* influence of the two pyrazolyl π-acceptor groups onto the *trans* metal–carbonyl bonds. Since in **3** and **4** the "carboxylate arm" is involved in the formation of a 7-ring instead of a 6-ring as in *fac*-[M(bdmpza)(CO)₃] (M = Mn, Re), the bonds are possibly less strained. This diminished strain results in bond angles around the metal ion, which are generally closer to an ideal octahedron than in tricarbonyl complexes with bpza or bdmpza as ligands and are rather similar to the angles in *fac*-[M(bmip)(CO)₃] (M = Mn, Re) [11]. It is noteworthy, that the distance between manganese and the carbonyl ligand *trans* to the carboxylate group [d(Mn1–C5) = 1.779(4) Å] is shorter than in both complexes *fac*-[Mn(bdmpza)(CO)₃] [1.804(4) Å] and *fac*-[Mn(bmip)(CO)₃] [1.800(3) Å] (Table 2). In both compounds **3** and **4** one molecule methanol co-crystallises per asymmetric unit. In both cases it forms a hydrogen bond to the oxygen atom O2 of the ligand [**3**: d(O2–O3) = 2.751 Å, **4**: d(O2–O31) = 2.778 Å].

The IR spectra of **3** and **4** show three bands (A′, A″ and A′), which are typical for a tricarbonyl complex with C_s symmetry. As expected, the manganese CO signals are found at slightly higher
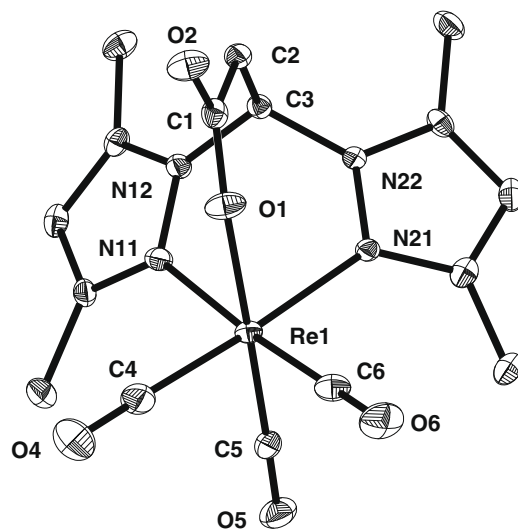

Fig. 4. Molecular structure of *fac*-[Re(bdmpzp)(CO)₃] (**4**); thermal ellipsoids are drawn at the 50% probability level.

Fig. 3. Molecular structure of *fac*-[Mn(bdmpzp)(CO)₃] (**3**); thermal ellipsoids are drawn at the 50% probability level.

Table 1
Selected bond distances (Å) and angles (°) of **3** and **4**.

	3	4
M1–N11	2.065(3)	2.170(3)
M1–N21	2.062(3)	2.177(3)
M1–O1	2.040(3)	2.128(3)
M1–C4	1.811(4)	1.936(4)
M1–C5	1.779(4)	1.896(4)
M1–C6	1.814(4)	1.915(4)
C1–C2	1.517(5)	1.520(6)
C1–O1	1.269(4)	1.269(5)
C1–O2	1.248(4)	1.233(5)
N11–M1–N21	85.8(1)	81.9(1)
O1–M1–N11	89.6(1)	86.3(1)
O1–M1–N21	89.3(1)	86.5(1)
O1–M1–C5	177.3(2)	179.4(1)
N21–M1–C4	176.7(2)	176.8(2)
N11–M1–C6	177.9(2)	175.9(2)
C4–M1–C5	91.1(2)	88.1(2)
C6–M1–C5	89.3(2)	89.8(2)
C4–M1–C6	85.9(2)	87.3(2)

wavenumbers than those of the rhenium complex. The carbonyl vibration frequencies of **3** and **4** are almost identical to those of the complexes *fac*-[Mn(bdmpza)(CO)$_3$] and *fac*-[Re(bdmpza)(CO)$_3$] (Table 3) [4,11]. These data confirm the result of the DFT calculations, that bdmpzp and bdmpza ligands have almost the same electronic properties.

Besides the *fac*-[M(CO)$_3$]$^+$-core (M = Re, Tc) the metal fragments *fac*-[M(CO)$_2$(NO)]$^{2+}$ and *fac*-[MO$_3$]$^+$ (M = Re, Tc) are subjects of current radiopharmaceutical research [6,8]. In the *fac*-[M(CO)$_2$-(NO)]$^{2+}$-core one of the carbonyl ligands is replaced by the isoelectronic [NO]$^+$ ligand. [NO]$^+$ is a stronger π-acceptor than CO and changes the charge of the complex by +1, thus creating a "harder" metal centre as compared to *fac*-[M(CO)$_3$]$^+$, which is commonly considered as "soft" [8]. Furthermore, due to its higher charge *fac*-[M(CO)$_2$(NO)]$^{2+}$ is assumed to possess a higher binding affinity to anionic chelating ligands that are frequently used as linkers between the metal core and biomolecules [16,17]. [Re(bdmpzp)-(CO)$_2$(NO)](BF$_4$) (**5**) is accessible from *fac*-[Re-(bdmpzp)(CO)$_3$] (**4**) and NOBF$_4$ in a ligand exchange reaction (Eq. (4)). This behaviour resembles closely that of *fac*-[Re(Cp)(CO)$_3$] and *fac*-[Re(bdmpza)(CO)$_3$] [4].
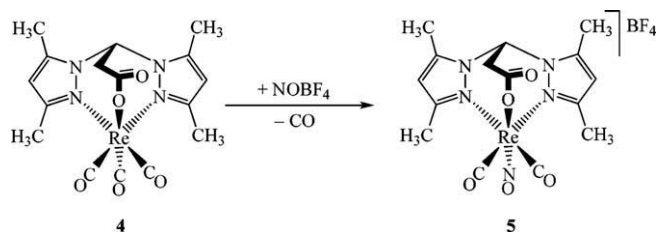
Eq. (4). Reaction of *fac*-[Re(bdmpzp)(CO)$_3$] (**4**) with NOBF$_4$.

In the ^{1}H and ^{13}C NMR spectra of **5** only one set of signals for the pyrazolyl groups is detected. This clearly indicates the existence of a mirror plane in the complex, which means that only the carbonyl ligand *trans* to the carboxylate group was substituted by a nitrosyl ligand. Remarkably, in the complex [Re(bdmpza)(CO)$_2$(NO)](BF$_4$) an entirely different result was found. There only the carbonyl ligands *trans* to the N donors were replaced by [NO]$^+$, thus resulting in a C_1 symmetry of the complex and two sets of signals for the pyrazole groups in the NMR spectra [10]. To find a possible explanation for this different behaviour, we performed DFT calculations on [Re(bdmpzp)(CO)$_2$(NO)]$^+$ and [Re(bdmpza)(CO)$_2$(NO)]$^+$. For each complex both isomers were considered, either with the nitrosyl ligand in *cis* or in *trans*-position towards the carboxylate group (Fig. 5).

According to the DFT calculations the arrangement of the nitrosyl ligand *trans* to the carboxylate group is energetically favoured by 28.24 kJ mol^{-1} in [Re(bdmpzp)(CO)$_2$(NO)]$^+$. For [Re(bdmpza)(CO)$_2$(NO)]$^+$ the *trans*-position of the nitrosyl ligand is also favoured, but only by 16.35 kJ mol^{-1}. The energy difference between the two isomers is clearly smaller. Obviously, the reaction of NO[BF$_4$] with *fac*-[Re(bdmpzp)(CO)$_3$] (**4**) at ambient temperature results in the thermodynamic product. A similar reaction with *fac*-[Re(bdmpza)(CO)$_3$] seems to favour the kinetic product [4]. So far the reason for these differences remains unclear.

The fact that the *trans*-arrangement of NO$^+$ and the carboxylate is energetically favoured in both cases, may be explained by the excellent π-acceptor properties of NO$^+$. If the nitrosyl ligand is situated *trans* to a pyrazolyl group, two ligands with π-acceptor properties compete for the electron density of the same metal d-orbital and hence mutually weaken their bonds to the metal. This effect is avoided when the nitrosyl ligand is arranged *trans* to the carboxylate group. A reason, why the difference is far more obvious for [Re(bdmpzp)(CO)$_2$(NO)]$^+$, may be indicated by the calculated structures of the complexes (Fig. 5). In [Re(bdmpzp)(CO)$_2$(NO)]$^+$, the carboxylate group can bend out of the mirror plane of the complex without stretching the metal-oxygen bond length. This bending of the carboxylate group leads almost to a *syn*-like instead of an *anti*-coordination of the carboxylate group towards the metal centre. According to calculations and stereochemical considerations the *syn* lone pair of a carboxylate group is regarded as more basic than the *anti* lone pair. The higher basicity is probably the reason why as well in enzymes as in many complexes a coordination via the *syn* lone pair is favoured [18].

Depending on the arrangement of the nitrosyl ligand in relation to the carboxylate group the electronical circumstances in the complexes are slightly different. These differences should be mirrored in the IR spectra. The IR spectra of **5** and [Re(bdmpza)(CO)$_2$(NO)][BF$_4$] were recorded in KBr (Table 4). Obviously, both spectra are quite similar. The differences which can be found are probably mainly due to the position of the CO and NO$^+$ ligands in relation to the pyrazolyl groups, which exert a *trans* influence on their opposite ligands.

In rhenium and technetium radiopharmaceutical research, both metal fragments, *fac*-[M(CO)$_3$]$^+$ and *fac*-[MO$_3$]$^+$, are interesting

Table 2
Metal–carbonyl distances of the complexes *fac*-[ML(CO)$_3$] (M = Mn, Re; L = bdmpza, bdmpzp, bmip).

Ligand	bdmpza [4]		bdmpzp		bmip [11]	
Distance (Å)	*trans* to N donor	*trans* to CO$_2^-$	*trans* to N donor	*trans* to CO$_2^-$	*trans* to N donor	*trans* to CO$_2^-$
d(Mn–CO)	1.819(4) 1.816(4)	1.804(4)	1.815(4) 1.811(4)	1.779(4)	1.836(3) 1.833(4)	1.800(3)
d(Re–CO)	1.96(1) 1.97(1)	1.94(1)	1.915(4) 1.936(4)	1.896(4)	1.953(6) 1.928(6)	1.899(6)

Table 3
Selected IR signals (cm^{-1}) of *fac*-[LMn(CO)$_3$] and *fac*-[LRe(CO)$_3$] (L = bdmpzp, bpza, bdmpza, bmip).

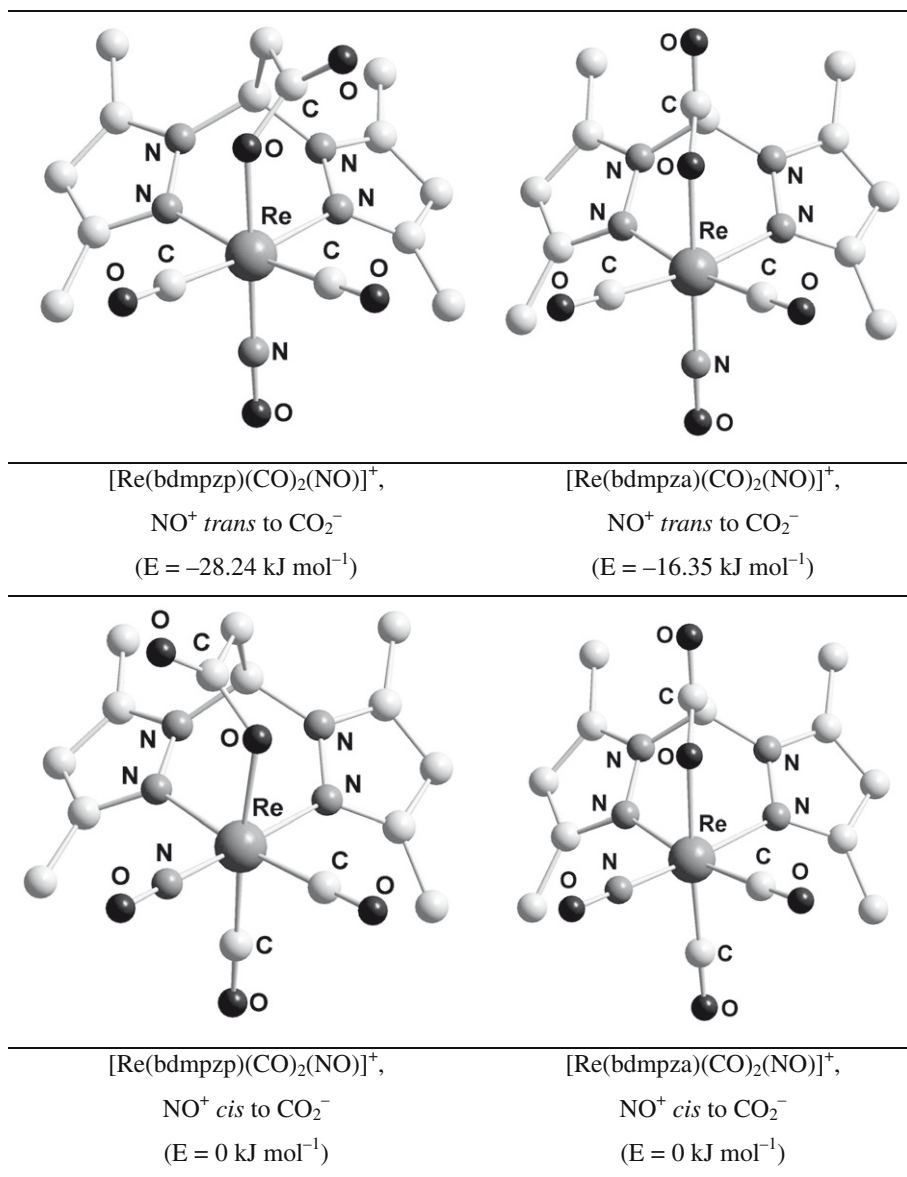| Ligand L	bdmpzp	bpza	bdmpza	bmip
$\bar{\nu}$(CO) (CH$_3$OH) *fac*-[LRe(CO)$_3$]	2029, 1922, 1902	–	2030, 1926, 1908 [11]	2023, 1914, 1896 [11]
$\bar{\nu}$(CO) (KBr) *fac*-[LRe(CO)$_3$]	2019, 1902	2028, 1922, 1906, 1895 [4]	2023, 1915, 1903, 1883 [4]	2018, 1898, 1867 [11]
$\bar{\nu}$(CO) (CH$_3$OH) *fac*-[LMn(CO)$_3$]	2039, 1946, 1923	2046, 1955, 1937 [4]	2041, 1949, 1927 [11]	2035, 1936, 1918 [11]
$\bar{\nu}$(CO) (KBr) *fac*-[LMn(CO)$_3$]	2032, 1940, 1924	2039, 1952, 1943, 1927, 1916 [4]	2036, 1924 [4]	2027, 1922, 1895 [11]

| | [Re(bdmpzp)(CO)$_2$(NO)]$^+$, NO$^+$ *trans* to CO$_2^-$ (E = –28.24 kJ mol^{-1}) | [Re(bdmpza)(CO)$_2$(NO)]$^+$, NO$^+$ *trans* to CO$_2^-$ (E = –16.35 kJ mol^{-1}) |
| [Re(bdmpzp)(CO)$_2$(NO)]$^+$, NO$^+$ *cis* to CO$_2^-$ (E = 0 kJ mol^{-1}) | [Re(bdmpza)(CO)$_2$(NO)]$^+$, NO$^+$ *cis* to CO$_2^-$ (E = 0 kJ mol^{-1}) |

Fig. 5. Calculated structures of [Re(bdmpzp)(CO)$_2$(NO)]$^+$ and [Re(bdmpza)(CO)$_2$(NO)]$^+$. The energies of the energetically higher isomers have been arbitrarily set to 0 kJ mol^{-1}.

Table 4
Comparison of the IR spectra of [Re(bdmpzp)(CO)$_2$(NO)][BF$_4$] (**5**) and [Re(bdmpza)(CO)$_2$(NO)][BF$_4$].

	$\tilde{v}$(CO)		$\tilde{v}$(NO)	$\tilde{v}$(as-CO$_2^-$)
[Re(bdmpzp)(CO)$_2$(NO)][BF$_4$](NO$^+$ *trans* CO$_2^-$)	2113	2064	1810	1719
[Re(bdmpza)(CO)$_2$(NO)][BF$_4$](NO$^+$ *cis* CO$_2^-$) [4]	2117	2044	1823	1706

cores for the labelling of receptor-targeting molecules. But compared to *fac*-[M(CO)$_3$]$^+$, the *fac*-[MO$_3$]$^+$ building block is smaller and hence expected to affect the binding properties of receptor-targeting biomolecules to a lower extent [6]. The complexes *fac*-[M(bdmpza)O$_3$] (M = Re, Tc) are already known [5,6]. To explore the binding properties of Hbdmpzp (**1**) further, the synthesis of *fac*-[Re(bdmpzp)O$_3$] was attempted. By analogy to the synthesis of *fac*-[Re(bdmpza)O$_3$], Hbdmpzp was reacted with HReO$_4$ (Eq. (5)).

The reaction yielded a white powder fairly soluble in polar organic solvents. All resonances in the ^{1}H NMR spectrum are shifted to slightly lower field in comparison to the free ligand **1**, and the coupling constants of the proton at the bridging carbon atom and of the CH$_2$ group are smaller [δ(CH$_{bridge}$) = 7.64 ppm, $^3J_{H,H}$ = 4.9 Hz,
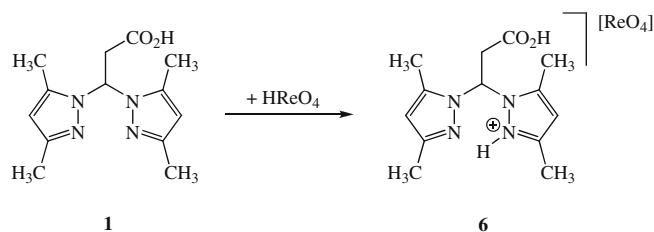
Eq. (5). Synthesis of [H$_2$bdmpzp][ReO$_4$] (**6**).

δ(CH$_2$) = 3.78 ppm, $^3J_{H,H}$ = 4.9 Hz]. The IR spectrum exhibits several intense bands, which can be assigned to Re=O-vibrations (926,

912, 903 cm^{-1}). A band at 1740 cm^{-1} was assigned to the carboxylate group. Since a coordinated carboxylate group usually appears at lower wavenumbers, these IR data were seen as a first hint that the reaction did not yield the complex *fac*-[Re(bdmpzp)O$_3$]. This suspicion was further supported by the result of the elemental analysis and eventually confirmed by an X-ray structure analysis (see Supporting Material).

This behaviour is clearly different from that of Hbdmpza and shows the limitations of the ligand Hbdmpzp. The synthesis of *fac*-[Re(bpzp)O$_3$] was attempted as well and yielded a white powder, but the product turned out to be very labile to hydrolysis. It is reasonably soluble only in DMSO, but the corresponding ^{1}H NMR spectrum showed only the ligand Hbpzp. When ^{1}H NMR spectra were recorded in CD$_3$CN, the quality of the spectra was poor. Two compounds could be discerned, though, and the signals of both were different from the spectrum of the free ligand **2**. Also the mass spectrum and the elemental analysis gave no hint to the formation of the desired product. The IR spectra of the product, which were recorded in KBr, showed some similarities to those of **6**. A carboxylate vibration was detected at 1747 cm^{-1}, furthermore a band at 1412 cm^{-1} and the Re=O-vibrations at 866, 908, 921 and 946 cm^{-1}. Therefore, also Hbpzp does not seem to be a suitable ligand for the *fac*-[ReO$_3$]$^+$-fragment.

3. Conclusion

Calculated dissociation energies seem to be apt to compare the influence of geometric alterations and electronic properties of different, but related ligands. All data are consistent with experimental results, especially IR data. Consequently, such calculations might allow an informed guess at the over-all properties of a new ligand even before it is synthesised. But when doing so, it has always to be borne in mind that the results of such calculations have to be interpreted cautiously. From IR spectra and X-ray data it became obvious that the complexes *fac*-[Mn(bdmpzp)(CO)$_3$] (**3**) and *fac*-[Re(bdmpzp)(CO)$_3$] (**4**) are closely related to similar complexes such as *fac*-[Mn(bdmpza)(CO)$_3$] and *fac*-[Re(bdmpza)(CO)$_3$]. The length of the "carboxylate arm" does not have a significant influence on the properties of the ligand. Hence, the large difference between bdmpza and bdmpzp on the one hand and bmip on the other hand can be attributed almost solely to the different *N* donor groups. Besides compounds **3** and **4**, also [Re(bdmpzp)-(CO)$_2$(NO)][BF$_4$] (**5**) was synthesised successfully. Compounds **4** and **5** might by useful for radiopharmaceutics research. The attempted synthesis of *fac*-[Re(bdmpzp)O$_3$] yielded [H$_2$bdmpzp]-[ReO$_4$] (**6**), instead.

4. Experimental

4.1. General

All operations were carried out under an inert gas atmosphere by using conventional Schlenk techniques. Solvents were freshly distilled and degassed prior to use from appropriate drying agents. The yields refer to analytically pure substances and were not optimised. IR spectra were recorded with a Varian Excalibur FTS-3500 FT-IR-spectrometer in CaF$_2$ cuvetts (d = 0.2 mm) or in KBr. ^{1}H and ^{13}C NMR spectra: Bruker DPX300 and Bruker DRX400, δ values relative to TMS or the deuterated solvent. Mass spectra were recorded on a Jeol JMS-700 using FD technique. Elemental analysis: Euro EA 3000 (Euro Vector) and EA 1108 (Carlo Erba). A Bruker-Nonius Kappa-CCD diffractometer and a STOE IPDS IIT diffractometer were used for X-ray structure determinations. [ReBr(CO)$_5$] and [MnBr(CO)$_5$] were synthesised according to literature [19,20].

4.2. Syntheses of the ligands

Hbdmpzp (**1**): To a solution of 3,5-dimethyl pyrazole (21.1 g, 220 mmol) in THF (200 mL), NaH (4.40 g, 60%, 110 mmol) is added portionwise and stirred at ambient temperature for 45 min. After addition of methyl propiolate (4.92 mL, 55.0 mmol, 1 equiv.) the mixture is heated to reflux for 48 h and subsequently stirred at ambient temperature for 60 h. The sodium salt of the product precipitates and forms a thick slurry, which is cooled to 0 °C and filtered. The residue is washed with ice-cold THF (5 × 40 mL) and subsequently dissolved in water. The solution is brought to pH 6 by addition of diluted HCl and extracted with diethyl ether (2 × 80 mL) to remove impurities. Subsequently, the aqueous phase is acidified to pH 2 and extracted with CH$_2$Cl$_2$ (6 × 100 mL). The combined CH$_2$Cl$_2$ phases are dried (Na$_2$SO$_4$), and the solvent is evaporated. The product is obtained as a white solid. Crystals suitable for an X-ray diffraction experiment were obtained from a solution in acetone.

Yield: 4.9 g (18.6 mmol, 34%). M.p.: 183–184 °C. ^{1}H NMR (CDCl$_3$, 300 MHz): δ = 2.13 (s, 6H, CH$_3$), 2.18 (s, 6H, CH$_3$), 3.63 (d, $^3J_{H,H}$ = 6.8 Hz, 2H, CH$_2$), 5.79 (s, 2H, CH$_{pz}$), 6.72 (t, $^3J_{H,H}$ = 6.8 Hz, 1H, CH$_{bridge}$) ppm. ^{1}H NMR (CD$_3$CN, 300 MHz): δ = 2.10 (s, 6H, CH$_3$), 2.25 (s, 6H, CH$_3$), 3.54 (d, $^3J_{H,H}$ = 6.8 Hz, 2H, CH$_2$), 5.81 (s, 2H, CH$_{pz}$), 6.58 (t, $^3J_{H,H}$ = 3.8 Hz, 1H, CH$_{bridge}$) ppm. ^{13}C NMR (CDCl$_3$, 75.5 MHz): δ = 10.9 (CH$_3$), 13.4 (CH$_3$), 39.2 (CH$_2$), 68.3 (CH$_{bridge}$), 107.3 (CH$_{pz}$), 140.1 (C–CH$_3$), 148.2 (C–CH$_3$), 171.2 (CO$_2$H) ppm. ^{13}C NMR (CD$_3$CN, 75.5 MHz): δ = 11.2 (CH$_3$), 13.6 (CH$_3$), 39.2 (CH$_2$), 67.2 (CH$_{bridge}$), 107.2 (CH$_{pz}$), 140.9 (C–CH$_3$), 148.7 (C–CH$_3$), 170.9 (CO$_2$H) ppm. EI MS: m/z (%) = 263 (50) [M+H$^+$], 166 (35) [M$^+$–C$_5$H$_7$N$_2$], 123 (80) [M$^+$–C$_5$H$_7$N$_2$–CO$_2$H], 96 (100) [C$_5$H$_7$N$_2$+H$^+$]. IR (THF): $\tilde{v}$ = 1735 s (*as*-CO$_2$H), 1560 m (C=N), 1419 w cm^{-1}. IR (KBr): $\tilde{v}$ = 1711 s (*as*-CO$_2$H), 1557 m (C=N), 1337 m, 1300 m, 1276 s cm^{-1}. Anal. Calc. for C$_{13}$H$_{18}$N$_4$O$_2$ (M = 262.31 g mol^{-1}): C, 59.53; H, 6.92; N, 21.36. Found: C, 59.61; H, 6.95; N, 21.51%.

Hbpzp (**2**): To a solution of pyrazole (10.0 g, 147 mmol) in THF (200 mL) NaH (2.93 g, 60%, 73.4 mmol) is added portionwise and stirred at ambient temperature for 1 h. After addition of methyl propiolate (3.28 mL, 36.7 mmol) the mixture is heated to reflux for 24 h. The solvent is evaporated, and the remaining solid is dissolved in 100 mL H$_2$O and brought to pH 7–8. The solution is extracted with diethyl ether (3 × 50 mL) to remove excess pyrazole and impurities. The aqueous phase is acidified to pH 2 by addition of diluted HCl and extracted with diethyl ether (6 × 100 mL). The combined organic phases are dried (Na$_2$SO$_4$), and the solvent is evaporated to yield the product as a yellow oil. After recrystallisation from acetone the product is obtained as colourless crystals suitable for an X-ray diffraction experiment.

Yield: 3.56 g (17.2 mmol, 47%). M.p.: 138–139 °C. ^{1}H NMR (DMSO-d_6, 300 MHz): δ = 3.66 (d, $^3J_{H,H}$ = 7.4 Hz, 2H, CH$_2$), 6.26 (vt, $^3J_{H,H}$ = 1.7 and 2.3 Hz, 2H, CH$_{pz}$), 6.93 (t, $^3J_{H,H}$ = 7.4 Hz, 1H, CH$_{bridge}$), 7.47 (d, $^3J_{H,H}$ = 1.3 Hz, 2H, CH$_{pz}$), 7.97 (d, $^3J_{H,H}$ = 2.5 Hz, 2H, CH$_{pz}$), 12.59 (s, br, 1H, CO$_2$H) ppm. ^{13}C NMR (DMSO-d_6, 75.5 MHz): δ = 37.6 (CH$_2$), 70.8 (CH$_{bridge}$), 106.0 (CH$_{pz}$), 129.5 (CH$_{pz}$), 139.5 (CH$_{pz}$), 170.0 (CO$_2$H) ppm. EI MS: m/z (%) = 207 (100) [M+H$^+$], 147 (85) [M$^+$–CO$_2$H–CH$_2$], 139 (65) [M$^+$–C$_3$H$_3$N$_2$], 95 (85) [M$^+$–CO$_2$H–C$_3$H$_3$N$_2$], 68 (70) [C$_3$H$_3$N$_2$+H$^+$]. IR (THF): $\tilde{v}$ = 1741 s (*as*-CO$_2$H), 1516 w (C=N), 1391 m cm^{-1}. IR (KBr): $\tilde{v}$ = 1709 s (*as*-CO$_2$H), 1520 w (C=N), 1434 m cm^{-1}. Anal. Calc. for C$_9$H$_{10}$N$_4$O$_2$ (M = 206.20 g mol^{-1}): C, 52.42; H, 4.89; N, 27.17. Found: C, 52.59; H, 4.96; N, 27.50%.

4.3. Syntheses of the complexes

fac-[Mn(bdmpzp)(CO)$_3$] (**3**): Potassium *tert*-butoxide (163 mg, 1.45 mmol) is added to a solution of Hbdmpzp (382 mg,

1.45 mmol) in THF (abs., 50 mL). The mixture is stirred at ambient temperature for 1 h. Subsequently [MnBr(CO)$_5$] (400 mg, 1.45 mmol) is added to the white suspension. The mixture is heated to 60 °C. The progress of the reaction can be monitored by IR spectroscopy. During the reaction the product precipitates as a yellow solid. Finally the supernatant is filtered off, and the yellow residue is washed with THF (3 × 30 mL), water (3 × 30 mL) and diethylether (3 × 10 mL) and dried in vacuo. The product is obtained as a yellow powder. Crystals suitable for an X-ray diffraction experiment were obtained from a solution in methanol/water.

Yield: 350 mg (0.874 mmol, 60%). M.p.: 199–201 °C (dec.). ^{1}H NMR (CDCl$_3$, 300 MHz): δ = 2.38 (s, 6H, CH$_3$), 2.64 (s, 6H, CH$_3$), 2.99 (s, br, 2H, CH$_2$), 6.11 (s, 2H, CH$_{pz}$), 6.21 (s, br, 1H, CH$_{bridge}$) ppm. ^{1}H NMR (DMSO-d_6, 400 MHz): δ = 2.44 (s, 6H, CH$_3$), 2.57 (s, 6H, CH$_3$), 2.85 (s, br, 2H, CH$_2$), 6.34 (s, 2H, CH$_{pz}$), 6.42 (s, br, 1H, CH$_{bridge}$) ppm. ^{13}C NMR (CDCl$_3$, 75.5 MHz): δ = 11.7 (CH$_3$), 15.7 (CH$_3$), CH$_2$-group not detected, 67.9 (CH$_{bridge}$), 108.9 (CH$_{pz}$), 141.2 (C–CH$_3$), 154.8 (C–CH$_3$), CO$_2^-$ and CO not detected, ppm. ^{13}C NMR (DMSO-d_6, 100.6 MHz): δ = 11.1 (CH$_3$), 15.2 (CH$_3$), 43.7 (CH$_2$), 63.4 (CH$_{bridge}$), 108.4 (CH$_{pz}$), 143.8 (C–CH$_3$), 155.4 (C–CH$_3$), CO$_2^-$ not detected, 220.9 (CO) ppm. FD MS: m/z (%) = 401 (100) [M+H$^+$]. IR (MeOH): $\tilde{v}$ = 2039 s, 1946 s, 1923 s (3 × CO), 1602 m (as-CO$_2^-$) cm^{-1}. IR (KBr): $\tilde{v}$ = 2028 s (CO), 1932 s, 1924 s, 1917 s (2 × CO), 1619 m (as-CO$_2^-$) cm^{-1}. Anal. Calc. for C$_{16}$H$_{17}$MnN$_4$O$_5$ (M = 400.27 g mol^{-1}): C, 48.01; H, 4.28; N, 14.00. Found: C, 48.00; H, 4.32; N, 13.97%.

fac-[Re(bdmpzp)(CO)$_3$] (**4**): Potassium *tert*-butoxide (83 mg, 0.739 mmol) is added to a solution of Hbdmpzp (194 mg, 0.739 mmol) in THF (abs., 40 mL). The mixture is stirred at ambient temperature for 1 h. Subsequently [ReBr(CO)$_5$] (300 mg, 0.739 mmol) is added to the white suspension. The mixture is heated to 60 °C. The progress of the reaction can be monitored by IR spectroscopy. During the reaction the product precipitates as a white solid. Finally the supernatant is filtered off, and the white residue is washed with THF (3 × 30 mL), water (3 × 30 mL) and diethylether (3 × 10 mL) and dried in vacuo. The product is obtained as a white powder. Crystals suitable for an X-ray diffraction experiment were obtained from a solution in methanol/water.

Yield: 303 mg (0.570 mmol, 77%). M.p.: 235–236 °C (dec.). ^{1}H NMR (CDCl$_3$, 300 MHz): δ = 2.42 (s, 6H, CH$_3$), 2.59 (s, 6H, CH$_3$), 3.16 (d, $^3J_{H,H}$ = 3.8 Hz, 2H, CH$_2$), 6.14 (s, 2H, CH$_{pz}$), 6.38 (t, $^3J_{H,H}$ = 3.8 Hz, 1H, CH$_{bridge}$) ppm. ^{1}H NMR (DMSO-d_6, 400 MHz): δ = signals of the CH$_3$-groups are superimposed by the solvent signal, 3.07 (s, br, 2H, CH$_2$), 6.38 (s, br, 2H, CH$_{pz}$), 6.57 (s, br, 1H, CH$_{bridge}$) ppm. ^{13}C NMR (CDCl$_3$, 75.5 MHz): δ = 11.7 (CH$_3$), 16.6 (CH$_3$), 44.2 (CH$_2$), 64.2 (CH$_{bridge}$), 108.6 (CH$_{pz}$), 141.4 (C–CH$_3$), 155.3 (C–CH$_3$), 172.1 (CO$_2^-$), CO not detected, ppm. ^{13}C NMR (DMSO-d_6, 100.6 MHz): δ = 11.2 (CH$_3$), 16.0 (CH$_3$), 44.5 (CH$_2$), 64.2 (CH$_{bridge}$), 108.1 (CH$_{pz}$), 144.1 (C–CH$_3$), 153.7 (C–CH$_3$), 171.4 (CO$_2^-$), 196.3 (CO), 196.5 (2 × CO) ppm. FD MS: m/z (%) = 533 (100) [M+H$^+$], 489 (15) [MH$^+$–CO$_2$]. IR (MeOH): $\tilde{v}$ = 2029 s, 1922 s, 1902 s (3 × CO), 1607 m (as-CO$_2^-$) cm^{-1}. IR (KBr): $\tilde{v}$ = 2019 s, 1902 s br (3 × CO), 1630 m (as-CO$_2^-$) cm^{-1}. Anal. Calc. C$_{16}$H$_{17}$N$_4$O$_5$Re (M = 531.54 g mol^{-1}): C, 36.15; H, 3.22; N, 10.54. Found: C, 35.79; H, 3.30; N, 10.40%.

[Re(bdmpzp)(CO)$_2$(NO)](BF$_4$) (**5**): *fac*-[Re(bdmpzp)(CO)$_3$] (300 mg, 0.564 mmol) is dissolved in CH$_2$Cl$_2$ (80 mL), and nitrosyl tetrafluoroborate (165 mg, 1.41 mmol) is added. The solution is stirred for three days at ambient temperature. During this time more nitrosyl tetrafluoroborate (412 mg, 3.53 mmol) is added portionwise. As the reaction proceeds, a light yellow precipitate is formed. After three days the solvent is removed in vacuo and the residue is dissolved in acetone (50 mL) to quench the excess NOBF$_4$. The acetone is evaporated. The residue is dissolved in THF (6 mL), and the product is precipitated with diethyl ether

(60 mL). After removal of the solvent the pale yellow precipitate is dried in vacuo.

Yield: 108 mg (0.175 mmol, 31%). M.p.: 156–158 °C. ^{1}H NMR (acetone-d_6, 300 MHz): δ = 2.70 (s, 6H, CH$_3$), 2.71 (s, 6H, CH$_3$), 3.78 (d, $^3J_{H,H}$ = 4.9 Hz, 2H, CH$_2$), 6.57 (s, 2H, CH$_{pz}$), 7.64 (t, $^3J_{H,H}$ = 4.9 Hz, 1H, CH$_{bridge}$) ppm. ^{13}C NMR (acetone-d_6, 100.6 MHz): δ = 11.7 (CH$_3$), 16.2 (CH$_3$), 41.6 (CH$_2$), 65.5 (CH$_{bridge}$), 111.3 (CH$_{pz}$), 147.2 (C–CH$_3$), 159.1 (C–CH$_3$), 170.7 (CO$_2^-$), 184.4 (2 × CO) ppm. FD MS: m/z (%) = 533 (100) [Re(bdmpzp)(NO)-(CO)$_2$]$^+$. IR (THF): $\tilde{v}$ = 2125 s (CO), 2066 s (CO), 1803 m (NO), 1725 w (CO$_2^-$), 1560 w (CN) cm^{-1}. IR (KBr): $\tilde{v}$ = 2123 s (CO), 2064 s (CO), 1810 s (NO), 1719 m (CO$_2^-$), 1561 m (CN) cm^{-1}. Anal. Calc. for C$_{15}$H$_{17}$BF$_4$N$_5$O$_5$Re × 2 CH$_2$Cl$_2$ (M = 790.20 g mol^{-1}): C, 25.84; H, 2.68; N, 8.86. Found: C, 25.55; H, 2.92; N, 9.55%.

[H$_2$bdmpzp][ReO$_4$] (**6**): Hbdmpzp (**1**) (787 mg, 3.00 mmol) was dissolved in acetonitrile (80 mL) and HReO$_4$ (985 mg of a 76.5% solution in water, 3.00 mmol) was added. The mixture was stirred at room temperature for 1 h. The solvent was reduced in vacuo and the product was precipitated with diethyl ether. The supernatant was removed and the white precipitate was dried in vacuo.

Yield: 1.21 g (2.44 mmol, 81%). M.p.: 138–139 °C (dec.). ^{1}H NMR (CD$_3$CN, 300 MHz): δ = 2.70 (s, 6H, CH$_3$), 2.71 (s, 6H, CH$_3$), 3.78 (d, $^3J_{H,H}$ = 4.9 Hz, 2H, CH$_2$), 6.57 (s, 2H, CH$_{pz}$), 7.64 (t, $^3J_{H,H}$ = 4.9 Hz, 1H, CH$_{bridge}$) ppm. ^{13}C NMR (CD$_3$CN, 75.5 MHz): δ = 11.4 (CH$_3$), 12.7 (CH$_3$), 39.1 (CH$_2$), 65.7 (CH$_{bridge}$), 108.6 (CH$_{pz}$), 145.2 (C–CH$_3$), 150.7 (C–CH$_3$), 169.7 (CO$_2^-$) ppm. FD MS: m/z (%) = 264 (15) [H$_2$bdmpzp+H$^+$], 246 (100) [H$_2$bdmpzp+H$^+$–H$_2$O]. IR (KBr): $\tilde{v}$ = 1740 m (CO$_2^-$), 1584 w (CN), 1563 vw, 1409 w, 1276 vw, 1240 vw, 1180 w, 1160 vw, 926 s, 912 s, 903 s (3 × Re=O) cm^{-1}. Anal. Calc. for C$_{13}$H$_{19}$N$_4$O$_6$Re (M = 513.52 g mol^{-1}): C, 30.41; H, 3.73; N, 10.91. Found: C, 30.46; H, 3.77; N, 10.98%.

4.4. DFT calculations

All DFT-calculations were carried out by using the Jaguar 6.0012 [21] software running on Linux 2.4.18-14smp on five Athlon MP 2800+ dual-processor workstations (Beowulf-cluster) parallelized with MPICH 1.2.4. MM2 optimised structures were used as starting geometries. Complete geometry-optimisations were carried out on the implemented LACVP* (Hay-Wadt ECP basis on heavy atoms, N31G6* for all other atoms) basis set and with the BP86 density functional. Orbital plots [22] were obtained using Maestro 7.0.113, the graphical interface of Jaguar. For the calculation of the dissociation energies the hybrid functional B3P86 was used.

4.5. X-ray structure determinations

Single crystals of **1**, **2**, **3**, **4** and **6** were mounted with protective Paratone-N or perfluoro polyalkylether oil on top of glass fibres. A Bruker-Nonius Kappa-CCD diffractometer and a STOE IPDS IIT diffractometer were used for data collection (graphite monochromator, Mo Kα radiation, λ = 0.71073 Å). The structures were solved by using direct methods and refined with full-matrix least squares against F^2 {Siemens SHELX-97} [23]. A weighting scheme was applied in the last steps of the refinement with $w = 1/[\sigma^2(F_o^2) + (aP)^2 + bP]$ and $P = [2Fc^2 + \max(F_o^2, 0)]/3$. In both compounds **3** and **4** one molecule methanol co-crystallises per asymmetric unit. In both cases it forms a hydrogen bond to the oxygen atom O2 of the ligand [**3**: d(O2–O3) = 2.751(1) Å, **4**: d(O2–O31) = 2.778 Å]. Most hydrogen atoms were included in their calculated positions and refined in a riding model. All details and parameters of the measurements are summarised in Tables 5 or the supporting material (Table S2). The structure pictures were prepared with the program Diamond 2.1e [24].

Table 5
Details of the structure determinations of the complexes **3** and **4**.

	fac-[Mn(bdmpzp)-(CO)$_3$] (**3**)	*fac*-[Re(bdmpzp)-(CO)$_3$] (**4**)
Empirical formula	C$_{16}$H$_{17}$MnN$_4$O$_5$ × CH$_3$OH	C$_{16}$H$_{17}$N$_4$O$_5$Re × CH$_3$OH
Formula weight	432.32	563.58
Crystal colour/habit	Yellow block	Colourless prism
Crystal system	Orthorhombic	Orthorhombic
Space group	*Pbca*	*Pbca*
a (Å)	14.759(3)	14.927(1)
b (Å)	9.982(2)	10.1077(2)
c (Å)	25.195(5)	25.162(2)
α (°)	90	90
β (°)	90	90
γ (°)	90	90
V (Å^3)	3711.9(13)	3796.4(4)
θ (°)	2.13–25.77	2.92–29.04
H	−18 to 17	−19 to 20
K	−12 to 12	−12 to 13
L	−30 to 30	−34 to 34
F(000)	1792	2192
Z	8	8
μ(Mo Kα) (mm^{-1})	0.755	6.444
Crystal size	0.3 × 0.2 × 0.1	0.37 × 0.18 × 0.18
D$_c$ (g cm^{-3})	1.547	1.972
T (K)	100(2)	150(2)
Reflections collected	37915	44961
Independent reflections	3515	5020
Observed reflections (>2*σI*)	2476	4319
Parameter	256	256
Weight parameter *a*	0.0350	0.0285
Weight parameter *b*	5.6509	10.0387
R$_1$ (observed)	0.0609	0.0273
R$_1$ (overall)	0.099	0.0355
wR$_2$ (observed)	0.1009	0.0714
wR$_2$ (overall)	0.1115	0.0737
Difference in peak/hole (e/Å^3)	0.305/−0.521	1.385/−2.369

Appendix A. Supplementary material

CCDC 703687, 703688, 703689, 703690 and 703691 contain the supplementary crystallographic data for **1**, **2**, **3**, **4** and **6**. These data can be obtained free of charge from The Cambridge Crystallographic Data Centre via www.ccdc.cam.ac.uk/data_request/cif. Supplementary data associated with this article can be found, in the online version, at doi:10.1016/j.jorganchem.2009.03.037.

References

[1] A. Otero, J. Fernández-Baeza, A. Tejeda, A. Antiñolo, F. Carillo-Hermosilla, E. Díez-Barra, A. Lara-Sánchez, M. Fernández-López, M. Lanfranchi, M.A. Pellinghelli, J. Chem. Soc., Dalton Trans. (1999) 3537.
[2] A. Otero, J. Fernández-Baeza, A. Antiñolo, J. Tejeda, A. Lara-Sánchez, Dalton Trans. (2004) 1499.
[3] C. Pettinari, R. Pettinari, Coord. Chem. Rev. 249 (2005) 663.
[4] N. Burzlaff, I. Hegelmann, B. Weibert, J. Organomet. Chem. 626 (2001) 16.
[5] N. Burzlaff, I. Hegelmann, Inorg. Chim. Acta 329 (2002) 147.
[6] Y. Tooyama, H. Braband, B. Spingler, U. Abram, R. Alberto, Inorg. Chem. 47 (2008) 257.
[7] E. Díez-Barra, J. Guerra, V. Hornillos, S. Merino, J. Tejeda, Tetrahedron Lett. 45 (2004) 6937.
[8] D. Rattat, A. Verbruggen, H. Schmalle, H. Berke, R. Alberto, Tetrahedron Lett. 45 (2004) 4089.
[9] T. Leyssens, D. Peeters, A.G. Orpen, J.N. Harvey, Organometallics 26 (2007) 2637.
[10] B. Schwenzer, J. Schleu, N. Burzlaff, C. Karl, H. Fischer, J. Organomet. Chem. 641 (2002) 134.
[11] L. Peters, E. Hübner, N. Burzlaff, J. Organomet. Chem. 690 (2005) 2009.
[12] A. Beck, B. Weibert, N. Burzlaff, Eur. J. Inorg. Chem. (2001) 521.
[13] I. Hegelmann, N. Burzlaff, Eur. J. Inorg. Chem. (2003) 409.
[14] L. Peters, N. Burzlaff, Polyhedron 23 (2004) 245.
[15] E. Hübner, G. Türkoglu, M. Wolf, U. Zenneck, N. Burzlaff, Eur. J. Inorg. Chem. (2008) 1226.
[16] U. Abram, R. Alberto, J. Braz. Chem. Soc. 17 (2006) 1486.
[17] S.S. Jurisson, J.D. Lydon, Chem. Rev. 99 (1999) 2205.
[18] R.L. Rardin, W.B. Tolman, S.J. Lippard, New J. Chem. 15 (1991) 417.
[19] E.W. Abel, G. Wilkinson, J. Chem. Soc. (1959) 1501.
[20] D. Vitali, F. Calderazzo, Gazz. Chim. Ital. 102 (1972) 587.
[21] Jaguar, Version 6.0, Schrödinger, LLC, New York, NY 2005.
[22] R. Stowasser, R. Hoffmann, J. Am. Chem. Soc. 121 (1999) 3414.
[23] G.M. Sheldrick, Acta Cryst. A64 (2008) 112.
[24] K. Brandenburg, M. Berndt, Diamond – Visual Crystal Structure Information System, Crystal Impact GbR, Bonn, Germany, 1999.;
For a Software Review see: W.T. Pennington, J. Appl. Crystallogr. 32 (1999) 1028.